Development of a Drift-Kinetic Simulation Code for Estimating Collisional Transport Affected by RMPs and Radial Electric Field

journal or publication title	Contributions to Plasma Physics
volume	56
number	6-8
page range	592-597
year	2016-06-24
URL	http://hdl.handle.net/10655/00012622

doi: https://doi.org/10.1002/ctpp.201610044

Development of a drift-kinetic simulation code for estimating collisional transport affected by RMPs and radial electric field

Ryutaro Kanno[1,2,*], **Masanori Nunami**[1,2], **Shinsuke Satake**[1,2], **Seikichi Matsuoka**[3], and **Hisanori Takamaru**[4]

[1] National Institute for Fusion Science, Toki 509-5292, Japan
[2] Department of Fusion Science, SOKENDAI (The Graduate University for Advanced Studies), Toki 509-5292, Japan
[3] Research Organization for Information Science and Technology, Kobe 650-0047, Japan
[4] Department of Computer Science, Chubu University, Kasugai 487-8501, Japan

Received XXXX, revised XXXX, accepted XXXX
Published online XXXX

Key words drift-kinetic simulation, collisional transport, resonant magnetic perturbation, radial electric field.

A drift-kinetic δf simulation code is developed for estimating collisional transport in quasi-steady state of toroidal plasma affected by resonant magnetic perturbations and radial electric field. In this paper, validity of the code is confirmed through several test calculations. It is found that radial electron flux is reduced by positive radial-electric field, although radial diffusion of electron is strongly affected by chaotic field-lines under an assumption of zero electric field.

1 Introduction

Understanding of the collisional transport properties in a perturbed magnetic field is important for the control of fusion plasma by employing resonant magnetic perturbations (RMPs) [1]. In recent tokamak experiments, RMPs have been used to mitigate edge localized modes (ELMs) [2]. ELMs were satisfactorily mitigated/suppressed by the RMPs reducing edge plasma pressure gradient. It was found interestingly [2] that the enhanced transport was fairly different from the theoretical estimate based on the field line diffusion derived by Rechester and Rosenbluth [3]. On the other hand, it was confirmed by a test particle simulation [4] that the field line diffusion model was applicable to the evaluations of both the electron and ion diffusion coefficients in a sufficiently ergodized region. Therefore, there is the following open question: why does the difference between the theoretical and experimental results occur? The modifications of field line diffusion have been proposed, but a clear answer to the question has not been obtained [1, 5]. An overview of the related theoretical/simulation studies is given in Ref. [6]. Although the drift-kinetic equation is known as a powerful tool for the estimation of collisional transport (neoclassical transport) in toroidal plasma including 3-dimensional field geometry [7, 8], it has rarely been used for the studies of the transport in RMP field.

In order to search for the answer, we reconsider the fundamental properties of the transport, based on the drift-kinetic equation in 5-dimensional phase space. For this purpose, we have started from examining dependences of the ion thermal diffusivity on several important parameters (the strength of RMPs, collisionality, *etc.*) by using a δf simulation code, KEATS [9, 10], which is programmed to solve the drift-kinetic equation. In our previous studies under an assumption of zero electric field [10], which is the same assumption as in Refs. [3, 4], we found the following three main results. 1) The radial thermal diffusivity χ_r in the simulation is close to the diffusivity $\chi_r^{\rm RR}$ derived by Ref. [3] if χ_r is evaluated in a temporary state of the guiding-centre distribution function f during an extremely short period $\Delta t \ll \omega_{\rm t}^{-1}$ around a time $t \lesssim \omega_{\rm t}^{-1} \ll \nu_{\rm eff}^{-1}$. Here $\omega_{\rm t}$ is the transit frequency and $\nu_{\rm eff}$ is the effective collision frequency. The initial condition of f in the simulations is set to $f = f_{\rm M}$, i.e., $\delta f = 0$, at time $t = 0$, where $f_{\rm M}$ is a Maxwellian. The temporary state relaxes finally to a quasi-steady state of f after being sufficiently exposed to Coulomb scatterings, $t \gtrsim \nu_{\rm eff}^{-1}$. Note that in the δf simulations in this

* Corresponding author E-mail: kanno@nifs.ac.jp, Phone: +81 572 58 2280, Fax: +81 572 58 2630

paper, it is physically meaningful to evaluate χ_r in the quasi-steady state rather than the temporary state, which is the same as in the neoclassical theory. 2) The diffusivity χ_r evaluated in the quasi-steady state is extremely small compared with $\chi_r^{\rm RR}$. 3) The diffusivity χ_r has almost the same parameter-dependence as $\chi_r^{\rm RR}$. The details are shown in Refs. [9, 10]. These results partly explain the difference, but one of the most important effects is ignored; it is an effect of radial electric field E_r.

In this paper, we report further improvements of KEATS code to include the effect of E_r on the transport, and show the results of test calculations. The scheme of the developing code is explained in the next section. Several tests are executed to check validity of the code in section 3. Finally, summary is given in section 4.

2 Two weight δf method solving the drift-kinetic equation

A guiding-centre distribution function, $f = f(t, \boldsymbol{x}, \mathcal{E}, v_\parallel)$, is separated into $f_{\rm M}$ and δf, i.e., $f = f_{\rm M} + \delta f$, where $f_{\rm M} = f_{\rm M}(\boldsymbol{x}, v) = n\{m/2\pi T\}^{3/2}\exp\{-mv^2/2T\}$ is a Maxwellian background and δf is a small perturbation from $f_{\rm M}$. Here $\mathcal{E} = mv^2/2 + e\Phi$ is the energy, e is the charge, $\boldsymbol{v}$ is the velocity, $v = v(\boldsymbol{x}, \mathcal{E}) = |\boldsymbol{v}|$, $v_\parallel = \boldsymbol{v}\cdot\boldsymbol{b}$, $\boldsymbol{b} = \boldsymbol{B}/B$, $B = |\boldsymbol{B}|$ and $\boldsymbol{B}$ is a magnetic field. In this paper, the number density n, temperature T and electrostatic potential Φ are supposed to be given functions of minor radius r, which are independent of time t. Here the minor radius r is defined by the label of closed magnetic surfaces of the unperturbed magnetic field $\boldsymbol{B}_0$, where $\boldsymbol{B} = \boldsymbol{B}_0 + \delta\boldsymbol{B}$ and $\delta\boldsymbol{B}$ is the RMP field. Validity of the supposition with respect to $\{n, T, \Phi\}$ is discussed in section 3. Applying the decomposition $f = f_{\rm M} + \delta f$ to the drift-kinetic equation, we have the following equation:

$$\frac{\rm D}{{\rm D}t}\delta f = \left\{\frac{\partial}{\partial t} + (\boldsymbol{v}_\parallel + \boldsymbol{v}_{\rm d})\cdot\frac{\partial}{\partial \boldsymbol{x}} + \dot{v}_\parallel\frac{\partial}{\partial v_\parallel} - C_{\rm T}\right\}\delta f = -\left\{\frac{\rm D}{{\rm D}t}f_{\rm M} - C_{\rm F}f_{\rm M}\right\}, \tag{1}$$

where $\dot{\boldsymbol{x}} = \boldsymbol{v} = \boldsymbol{v}_\parallel + \boldsymbol{v}_{\rm d}$, $\dot{\mathcal{E}} = 0$ and $\dot{v}_\parallel = \boldsymbol{B}^*\cdot\{(e/m)\boldsymbol{E}_r - (\mu/m)\nabla B\}/B_\parallel^*$ [11, 12]. Here $\boldsymbol{v}_\parallel = v_\parallel\boldsymbol{B}^*/B_\parallel^*$ is the parallel velocity, $\boldsymbol{v}_{\rm d} = \{\boldsymbol{E}_r\times\boldsymbol{b} + (\mu/e)\boldsymbol{b}\times\nabla B\}/B_\parallel^*$ is the drift velocity, $\boldsymbol{E}_r$ is the radial electric field, $\mu = m{v_\perp}^2/2B$ is the magnetic moment, $v_\perp = \sqrt{v^2 - {v_\parallel}^2}$, $\boldsymbol{B}^* = \boldsymbol{B} + (mv_\parallel/e)\nabla\times\boldsymbol{b}$ and $B_\parallel^* = \boldsymbol{b}\cdot\boldsymbol{B}^*$. The Coulomb collision operator is described by $C_{\rm T}$ and $C_{\rm F}$, where $C_{\rm T}$ is the test-particle collision operator which represents the pitch-angle scattering and $C_{\rm F}$ is the field-particle collision operator which ensures local momentum conservation property [9]. Note that $\mathcal{E} = \mathrm{constant}$ in this simulation code. Effects of impurities and neutrals on the collisional transport are ignored in this paper.

To solve Eq. (1) by Monte-Carlo techniques, we adopt the two-weight scheme of the δf method [13]:

$$\frac{{\rm D}g}{{\rm D}t} = 0, \tag{2}$$

$$\frac{{\rm D}p}{{\rm D}t} = \frac{p}{f_{\rm M}}\frac{{\rm D}f_{\rm M}}{{\rm D}t}, \tag{3}$$

$$\frac{{\rm D}w}{{\rm D}t} = -\frac{{\rm D}p}{{\rm D}t} + \frac{p}{f_{\rm M}}C_{\rm F}f_{\rm M}, \tag{4}$$

where g is the marker distribution function and both p and w are the weight functions satisfying $pg = f_{\rm M}$ and $wg = \delta f$. The Monte-Carlo simulation code, KEATS, is based on the above method, and it seeks a quasi-steady state of δf satisfying Eq. (1) under the assumption of a given electric field. The code is programmed in the so-called helical coordinates (u^1, u^2, u^3), i.e., $\boldsymbol{x} = {}^{\rm t}(u^1, u^2, u^3)$ [14]. In this simulation code, the radial particle and energy fluxes are evaluated by the following equations, respectively:

$$\Gamma_r = \overline{\left\langle\nabla r\cdot\int {\rm d}^3v\,\boldsymbol{v}\,\delta f\right\rangle} \quad\text{and}\quad Q_r = \overline{\left\langle\nabla r\cdot\int {\rm d}^3v\,\frac{mv^2}{2}\boldsymbol{v}\,\delta f\right\rangle}, \tag{5}$$

where radial heat flux is given as $q_r = Q_r - (5/2)T\Gamma_r$. Here $\bar{\cdot}$ means the time-average. The time-averaging is carried out in the quasi-steady state of δf after sufficient exposure to Coulomb collisions. Another average $\langle\cdot\rangle$ is defined as $\langle\cdot\rangle = (1/\delta\mathcal{V})\int_{\delta\mathcal{V}}\cdot\,{\rm d}^3x$, where $\delta\mathcal{V}$ is a small volume and lies between two neighbouring reference surfaces with volumes $\mathcal{V}(r)$ and $\mathcal{V}(r) + \delta\mathcal{V}$. Note that a reference surface is labelled by r.

3 Test calculations

The toroidal magnetic configuration used in test calculations of the present code is given by the addition of an RMP field $\delta\boldsymbol{B}$ to a circular tokamak field $\boldsymbol{B}_0$, where the total magnetic field is $\boldsymbol{B} = \boldsymbol{B}_0 + \delta\boldsymbol{B}$. The unperturbed magnetic field $\boldsymbol{B}_0 = B_{0R}\widehat{R} + B_{0\varphi}\widehat{\varphi} + B_{0Z}\widehat{Z}$ is defined by $B_{0R} = -B_{\rm ax}Z/qR$, $B_{0\varphi} = -B_{\rm ax}R_{\rm ax}/R$ and $B_{0Z} = B_{\rm ax}(R - R_{\rm ax})/qR$, where $\widehat{R}$, $\widehat{\varphi}$ and $\widehat{Z}$ are the unit vectors in the R, φ and Z directions of the cylindrical coordinate system, respectively. Here q is the safety factor given as $q^{-1} = 0.9 - 0.5875(r/a)^2$, the major radius of the magnetic axis is set to $R_{\rm ax} = 3.6$ m, the minor radius of the toroidal plasma is $a = 1$ m and the strength of the magnetic field on the magnetic axis is $B_{\rm ax} = 4$ T. The RMPs causing resonance with rational surfaces of $q = k/\ell = 3/2, 10/7, 11/7, 13/9, 14/9, 16/11, 17/11, 19/13, 20/13, 22/15, 23/15, 25/17, 26/17$ are given by a perturbation field $\delta\boldsymbol{B} = \nabla \times (\alpha\boldsymbol{B}_0)$. The function α is given as $\alpha = \sum_{k,\ell} a_{k\ell}\cos\{k\theta - \ell\varphi\}$, which is a similar presupposition to one in Ref. [4]. Here $a_{k\ell} = A_{\rm RMP}\exp\{-(r - r_{k\ell})^2/\Delta r^2\}$ and $r = r_{k\ell}$ is the rational surface of $q = k/\ell$. We set the parameter $A_{\rm RMP} = 10^{-3}$ and $\Delta r/a = 5 \times 10^{-2}$ so that neighbourhood of resonant surfaces become ergodized. The perturbed region is bounded radially on both sides by the closed magnetic surfaces, and the centre of the perturbed region is around $r/a = 0.6$, as shown in Fig. 1. This RMP field is applied to the test calculations in subsection 3.2. Note the following points. In order to investigate the properties of the transport affected by only RMP field (i.e., to compare the simulation results with the theory of *field line diffusion*), the perturbed region is sufficiently away from the plasma edge $r/a = 1$, because there is a possibility that the particle orbit-loss at the plasma edge influences the transport. The RMPs should be selected to suit well to the comparison, as used in Ref. [4].

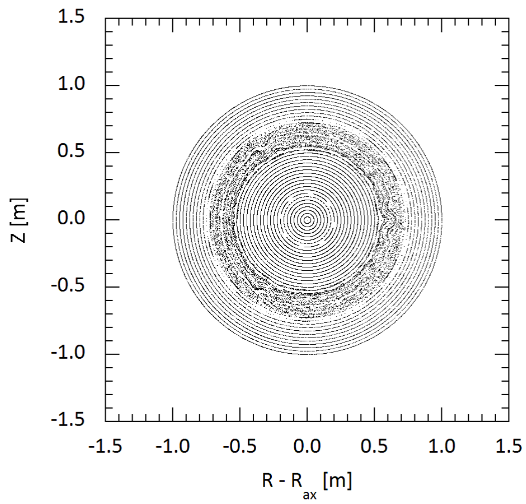

Fig. 1 Poincaré plot of the magnetic field lines on a poloidal cross section. Ergodized region is bounded radially on both sides by the closed magnetic surfaces (see $0.4 < r/a < 0.8$), and the centre of the perturbed region is around $r/a = 0.6$.

3.1 Self-consistent electric field in unperturbed magnetic field

In section 3, we attempt to confirm the validity of the code through several test calculations. First, the following drift-kinetic equation of ion is considered in case of $\delta\boldsymbol{B} = 0$.

$$\left\{\frac{\partial}{\partial t} + \boldsymbol{v}\cdot\frac{\partial}{\partial \boldsymbol{x}} - \frac{e\nabla\Phi}{m}\cdot\frac{\partial}{\partial \boldsymbol{v}}\right\} f = Cf, \tag{6}$$

where C is the Coulomb collision operator and $Cf = C(f, f)$ is the self-collision term. If $f = f_{\rm M}$ and $T = \mathrm{constant}$, then the following is derived from Eq. (6): $n\exp\{e\Phi/T\} = \mathrm{constant}$. Therefore, the radial electric field is self-consistently given as $E_r = (T/e)\,\mathrm{d}\ln n/\mathrm{d}r$, and both particle and energy fluxes are estimated as $\Gamma_r = 0$ and $Q_r = 0$, respectively. Here the density n is assumed to be a function of r. In this case, $\delta f = 0$ should be always satisfied if the initial condition is set to $\delta f = 0$ at time $t = 0$. This test calculation was carried out with the number of markers equal to 1.6×10^7. As shown in Fig. 2, the particle flux with the above electric field is confirmed as $\Gamma_r \approx 0$ during the simulation by the present code, and the energy flux is also evaluated as

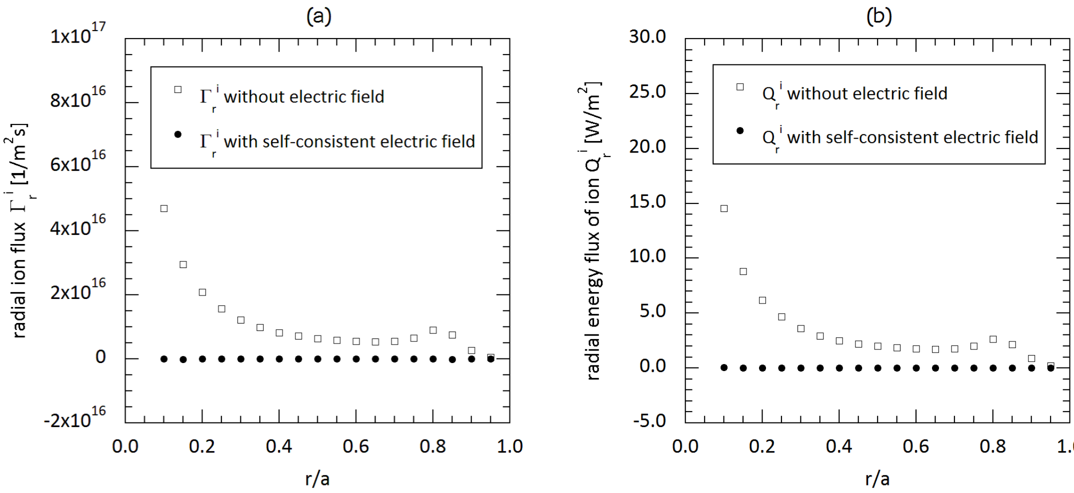

Fig. 2 Profiles of (a) radial particle flux $\varGamma_r$ and (b) radial energy flux Q_r in the unperturbed magnetic field, where $n = n_{\rm ax}\{1 - 0.2(r/a)\}$, $n_{\rm ax} = 1 \times 10^{19}$ m^{-3} and $T = 1$ keV. If electric field is ignored, then the self-collision-driven fluxes, $\varGamma_r$ and Q_r, are seen (open squares). On the other hand, when considering the self-consistent electric field, $\varGamma_r$ and Q_r vanish as expected (closed circles).

$Q_r \approx 0$. On the other hand, under the assumption of zero electric field, the self-collision-driven fluxes are seen. See also Refs. [15, 16].

3.2 Dependence of particle flux on radial electric field in an ergodized region

When adding RMP field on a circular tokamak field, magnetic flux surfaces around resonant surfaces of $q = k/\ell$ become often chaotic in the perturbed region, as shown in Fig. 1. In the present code, reference surfaces are defined by closed magnetic surfaces of $\boldsymbol{B}_0$, and thus the reference surfaces are labelled by minor radius r. The density n, temperature T and electrostatic potential $\varPhi$ are supposed to be given functions of minor radius r, and thus the dot product of the RMP field $\delta\boldsymbol{B}$ and the gradient of $\{n, T, \varPhi\}$ is not zero in general, i.e., $\boldsymbol{B} \cdot \nabla\{n, T, \varPhi\} = \delta\boldsymbol{B} \cdot \nabla\{n, T, \varPhi\} \neq 0$. Validity of this supposition is confirmed by the facts that after several collision times, 1) quasi-steady state of δf is finally found in the simulations and 2) the condition of $|\delta U/U| := |\overline{\langle \int {\rm d}^3 v (mv^2/2)\delta f\rangle}/(3nT/2)| \ll 1$ is satisfied in the perturbed region in the quasi-steady state, i.e.,

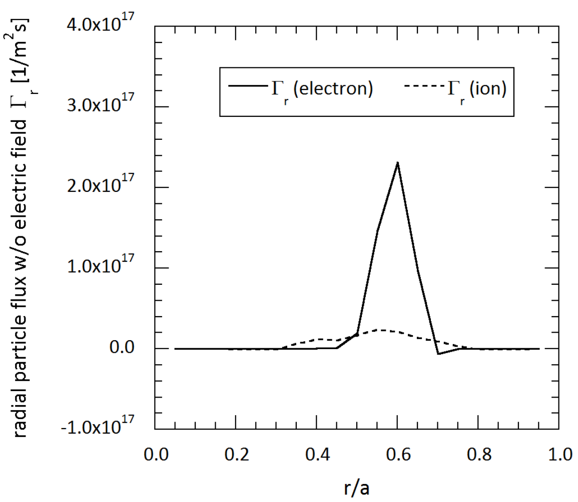

Fig. 3 Radial particle fluxes of electron (solid line) and ion (dashed line) in RMP field under the assumption of zero electric field. It is seen that $\varGamma_r^{\rm e} \gg \varGamma_r^{\rm i}$.

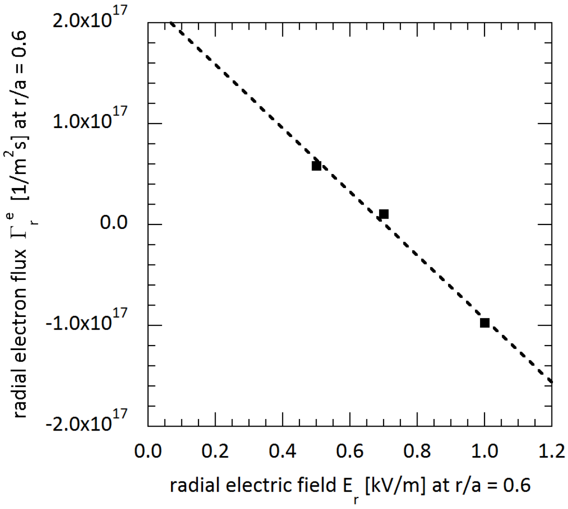

Fig. 4 Dependence of radial electron flux $\Gamma_r^{\rm e}$ on the radial electric filed at the centre of the perturbed region, i.e., $r/a \approx 0.6$. $\Gamma_r^{\rm e}$ is decreased by positive E_r and vanishes for $E_r \approx +0.7$ kV/m. A linear regression line is shown by the dashed line.

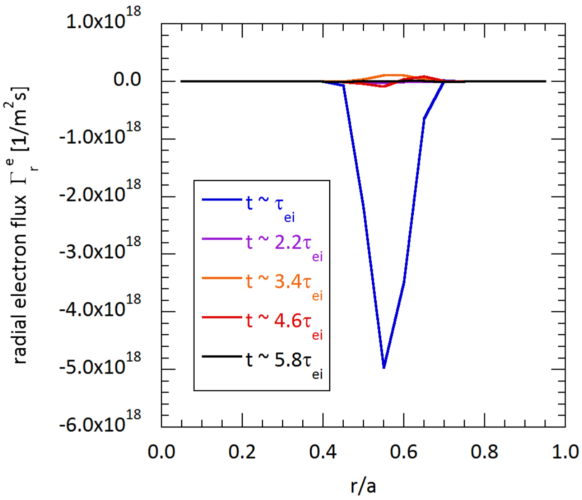

Fig. 5 Profiles of radial electron flux $\Gamma_r^{\rm e}$ for various time slices in case of $E_r(r/a = 0.6) \approx +0.7$ kV/m. $\Gamma_r^{\rm e}$ relaxes to negligibly small value in the quasi-steady state of δf after several times of the electron-ion collision time $\tau_{\rm ei}$.

$|\delta U/U| \lesssim 10^{-3}$ in the simulations. In this case, the calculations were carried out with the number of markers equal to 6.4×10^7.

Hereafter, we focus on the collisional transport in the perturbed region, then the density and temperature are given as $n/n_0 = T/T_0 = \{1 - 0.2(r/a)\}$ if $0.4 \leq r/a \leq 0.8$, $n/n_0 = T/T_0 = 0.92$ if $r/a < 0.4$, and $n/n_0 = T/T_0 = 0.84$ if $r/a > 0.8$, where $n_0 = 1.137 \times 10^{19}$ m^{-3} and $T_0 = 1.137$ keV. Here the density and temperature at the centre of the perturbed region are $n \approx 1 \times 10^{19}$ m^{-3} and $T \approx 1$ keV, respectively. The electrostatic potential in this case is modelled as $\Phi = -(\Phi_0/12)[\tanh\{12(r - 0.6a)/a\} - 1]$. The radial electric field at $r/a = 0.6$ is given as $E_r = \Phi_0/a$. Note that radial particle/heat fluxes and radial electric field are zero outside of the perturbed region.

By estimating radial particle fluxes of electron and ion under the assumption of zero electric field, it is found that the electron flux is much larger than the ion flux, i.e., $\Gamma_r^{\rm e} \gg \Gamma_r^{\rm i}$, because of chaotic field-lines, as shown in Fig. 3. Note that positive radial-electric-field is expected to satisfy the ambipolar condition, $\Gamma_r^{\rm e} = \Gamma_r^{\rm i}$, from this result. Therefore, we preliminary investigate dependence of electron flux on radial electric field E_r and evaluate the value of E_r when $\Gamma_r^{\rm e} \approx 0$. We find that the electron flux is reduced by radial electric field, as shown in Fig. 4, and that $\Gamma_r^{\rm e} \approx 0$ is satisfied in case of $E_r \approx +700$ V/m at the centre of the perturbed region, i.e., $r/a \approx 0.6$. Here we confirm that the radial electron flux in case of the model potential with $\Phi_0 \approx 700$ V (i.e., $E_r \approx +700$ V/m at $r/a = 0.6$) becomes negligibly small in the quasi-steady state of δf after being sufficiently exposed to Coulomb scatterings, $t \gg \tau_{\rm ei}$ ($\tau_{\rm ei}$ is the electron-ion collision time), as shown in Fig. 5.

4 Summary

We have improved the drift-kinetic δf simulation code KEATS for estimating collisional transport affected by RMPs and radial electric field. Several test calculations are attempted in the first trial, and the validity of the code for seeking a quasi-steady state of δf is confirmed. It is found that the radial electron flux strongly affected by RMPs is reduced by positive radial-electric-field. Estimation of radial particle and heat transport of both electron and ion, which is based on the drift-kinetic δf simulation satisfying $\Gamma_r^{\mathrm{e}} = \Gamma_r^{\mathrm{i}}$ in the perturbed region, and furthermore comparison between the simulation results and the theory of Ref. [3] are not executed in this first report on our code development, and these will be described elsewhere in the near future.

Acknowledgements The simulations in this paper were conducted using the supercomputers “Plasma Simulator” at National Institute for Fusion Science (NIFS) and “Helios” at International Fusion Energy Research Centre - Computational Simulation Centre (IFERC-CSC). This work was performed with the support and under the auspices of the NIFS Collaborative Research Programs “NIFS13KNST060” and “NIFS15KNST076” and the IFERC-CSC projects “PETAMP3” and “PETAMP4.”

References

[1] R. J. Hawryluk *et al.*, Nucl. Fusion **49**, 065012 (2009).
[2] T. E. Evans *et al.*, Nature Phys. **2**, 419 (2006).
[3] A. B. Rechester and M. N. Rosenbluth, Phys. Rev. Lett. **40**, 38 (1978).
[4] A. H. Boozer and R. B. White, Phys. Rev. Lett. **49**, 786 (1982).
[5] T. M. Wilks, W. M. Stacey and T. E. Evans, Phys. Plasmas **20**, 052505 (2013).
[6] S. Abdullaev, *Magnetic Stochasticity in Magnetically Confined Fusion Plasmas* (Springer, Cham, 2014) §10.5.
[7] M. Yokoyama *et al.*, Fusion Sci. Technol. **58**, 269 (2010).
[8] A. Briesemeister *et al.*, Plasma Phys. Control. Fusion **55**, 014002 (2013).
[9] R. Kanno *et al.*, Plasma Phys. Control. Fusion **52**, 115004 (2010).
[10] R. Kanno *et al.*, Plasma Phys. Control. Fusion **55**, 065005 (2013).
[11] R. G. Littlejohn, J. Plasma Phys. **29**, 111 (1983).
[12] P. Helander and D. J. Sigmar, *Collisional Transport in Magnetized Plasmas* (Cambridge Univ. Press, Cambridge, 2002) Chap. 6.
[13] W. X. Wang *et al*, Plasma Phys. Control. Fusion **41**, 1091 (1999).
[14] S. Jimbo *et al.*, Nucl. Fusion **45**, 1534 (2005).
[15] W. X. Wang *et al*, Phys. Rev. Lett. **87**, 055002 (2001).
[16] M. Okamoto *et al.* J. Plasma Fusion Res. SERIES **6**, 148 (2004).